利用T1定量图谱测定体模钆塞酸二钠溶液浓度并探索其最佳扫描序列

董 帜，冯艳青，王 猛，蔡华崧，李子平，冯仕庭，彭振鹏
（中山大学附属第一医院放射诊断专科，广东 广州 510080）

摘 要：【目的】评估利用T1Mapping(T1定量图谱)T1值测定体模钆塞酸二钠(Gd-EOB-DTPA)溶液浓度的准确性，确定较优的扫描序列。【方法】制备不同浓度(0.007-1.814 g/L)的Gd-EOB-DTPA溶液体模(n=12)并行MRI扫描。扫描序列包括T1加权(T1WI)序列(opp-phase、IR、SE、T1-fl2d、T1-vibe、T1-3D)及T1定量图谱(T1Mapping)序列(VIBE_Mapping、T1-tra-3D_Mapping、T1-fl2d_Mapping)。在T1WI中测量体模溶液Sp及同层参照物Sm，计算信噪比(SNR)(Sp/Sm)。在T1Mapping测量体模溶液T1p、同层参照物T1m，背景T1n，计算SNR =T1p/T1 n、对比噪声比(CNR)=|T1p-T1m|/T1n。【结果】除SE序列外(P=0.058)，其余各序列测定的信号强度(SI)、相对信号强度(RSI)与对比剂浓度分布均呈正相关(P<0.05)。体模溶液T1值与Gd-EOB-DTPA浓度分布呈负相关，相关性均有统计学意义(P<0.05)。T1Mapping序列中，VIBE序列的SNR、CNR高于T1-tra-3D、T1-fl2d(P<0.05)，T1-tra-3D与T1-fl2d的SNR、CNR差别无统计学意义(P>0.05)。【结论】T1Mapping软件可获得准确的T1值。VIBE序列所得T1Mapping图像质量高，扫描速度快，更适用于Gd-EOB-DTPA肝脏增强MR检查。

关键词：T1定量图谱；钆塞酸二钠；磁共振成像；体模
中图分类号：R445.2 **文献标志码：**A **文章编号：**1672-3554(2020)06-0867-08

Quantitative Gd-EOB-DTPA Concentration Using T1Mapping and to Explore the Best Scanning Sequence

DONG Zhi, FENG Yan-qing, WANG Meng, CAI Hua-song, LI Zi-ping, FENG Shi-ting, PENG Zhen-peng
(Department of Radiology, the First Affiliated Hospital, Sun Yat-sen University, Guangzhou 510080, China)
Correspondence to: PENG Zhen-peng; E-mail: 37595198@qq.com

Abstract: 【Objective】To evaluate the accuracy of the T1Mapping sequence in determining the concentration of the Gd-EOB-DTPA solution by measuring the T1values of the phantom, and to determine a better scanning sequence. 【Methods】Gd-EOB-DTPA solution phantom was prepared with different concentrations (0.007-1.814 g/L) for MRI scanning(n=12). Scanning sequences include T1weighted image (WI) sequences (opp-phase, IR, SE, T1-fl2d, T1-vibe, T1-3D) and T1Mapping sequences (VIBE_Mapping, T1-tra-3D_Mapping, T1-fl2d_Mapping). In T1WI, the signal intensity of the phantom solution (Sp) and that of the reference object (Sm) at the same level were measured, and the signal to noise ratio (SNR) (Sp/Sm) was calculated. In T1Mapping, the T1 values of the phantom solution (T1p), the reference at the same level (T1m) and the background (T1n) were measured respectively, and the SNR and contrast to noise ratio (CNR) were calculated (SNR=T1p/T1n, CNR=|T1p-T1m|/T1n). 【Results】The signal intensity(SI) and relative signal intensity (RSI) determined by the conventional sequences were positively correlated with the concentration of Gd-EOB-DTPA (P<0.05), except for the SE sequence (P=0.058). The T1 values of the phantom were negatively correlated with the concentration of Gd-EOB-DTPA, with statistically significance (P<0.05). Among the T1Mapping sequences,

收稿日期：2020-08-15
基金项目：国家自然科学基金(81971684，81771908，81770654)
作者简介：董帜，硕士，主治医师，研究方向：磁共振成像，E-mail：dongzh7@mail.sysu.edu.cn；彭振鹏，通信作者，副主任医师，研究方向：磁共振成像，E-mail：37595198@qq.com

the SNR and CNR of the VIBE sequence were higher than those of T1-tra-3D and T1-fl2d sequences (P<0.05). There was no statistically significant difference between T1-tra-3D and T1-fl2d sequences (P>0.05).【Conclusion】T1Mapping software can obtain accurate T1 values. The T1Mapping image obtained by the VIBE sequence has high quality and fast scanning speed, which is more suitable for Gd-EOB-DTPA enhanced MR examination of liver.

Key words: T1Mapping; Gd-EOB-DTPA; magnetic resonance imaging; phantom

[J SUN Yat-sen Univ(Med Sci),2020,41(6):867-874]

钆塞酸二钠(Gd-EOB-DTPA)是一种肝细胞特异性MRI对比剂,已广泛应用于肝脏结节的诊断与鉴别诊断[1-4],并开始应用于肝功能的评价[5]。Gd-EOB-DTPA被肝细胞摄取的情况可以用肝脏信号强度或T1定量图谱(T1 mapping)测量。由于组织信号强度的高低受很多因素影响,如脉冲序列、成像参数等,因此可能会带来误差[6-7]。而弛豫是组织的固有特性,在主磁场强度固定的情况下,其T1值基本保持稳定,故在相同的主场强B0下得到的T1值可以直接比较[6-7]。目前已有学者测定肝脏T1弛豫时间并应用于肝功能的评估,但由于其测量所得结果亦存在差异[7-9]。因此选择最佳的扫描序列,快速获得T1弛豫时间并准确测定是急需解决的问题。本研究拟用体模实验方法验证应用T1定量图谱软件测量T1值的准确性,并与目前应用较多的信号强度测量法进行对比,比较两种方法的各自的特点及其准确性,筛选出较优的扫描序列,为进一步临床应用提供依据。

1 材料与方法

1.1 体模制作

参照Friedman等[10]的研究方法制作体模。将1支(10mL)Gd-EOB-DTPA对比剂溶于1L蒸馏水中,得到浓度约为1.814 g/L的磁共振对比剂Gd-EOB-DTPA,再用蒸馏水稀释成12种不同浓度,分装于每支容量为15 mL的硬塑料试管中,再集中摆放于统一体模托架中。Gd-EOB-DTPA与蒸馏水稀释比例及溶液浓度见表1(图1)。试管管径1.5 cm,高12 cm。每支试管内稀释后总的溶液量为10 mL,从试管1到12溶液浓度渐次减低,相邻两支试管之间的稀释比为0.6。

表1 体模溶液稀释比例及Gd-EOB-DTPA浓度

Table 1 Dilution rate and Gd-EOB-DTPA concentration of the phantom

Number	1	2	3	4	5	6	7	8	9	10	11	12
Dilution rate	10‰	6‰	3.6‰	2.16‰	1.39‰	0.78‰	0.467‰	0.280‰	0.168‰	0.101‰	0.061‰	0.036‰
Concentration/(g/L)	1.814	1.088	0.653	0.392	0.235	0.141	0.085	0.051	0.030	0.018	0.011	0.007

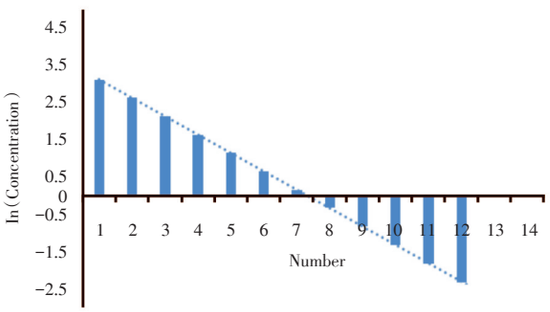

图1 Gd-EOB-DTPA溶液浓度分布

Fig.1 Concentration of Gd-EOB-DTPA solution

1.2 扫描方案

检查设备为Magnetom Verio 3.0T超导MRI(Siemens Heahhcare Sector, Erlangen, Germany),操作系统版本syngo MB17;使用8通道相控阵体线圈。

实验采用健康志愿者踝关节肌肉作为参照物对比测量信号强度。扫描时志愿者取左侧卧位,左腿屈曲,右腿伸直。体模托架与健康志愿者右侧踝关节并列排放,长轴位于磁场中心并与主磁场平行,保证体模与踝关节处于同一水平。体模内液面保持于同一水平。首先获得体模横、冠、矢

状位三个方向T1WI图像（FLASH序列，层厚3 mm，层间距1 mm，反转时间（reversetime，TR）：100 ms，回波时间（echo time，TE）：2.5 ms，翻转角70°），然后对体模溶液中部扫描。扫描序列及参数见表2，包含常用的T1WI扫描序列以及能应用该MRI设备所提供的T1Mapping软件的T1WI扫描序列。

利用Magnetom Verio 3.0T超导MRIT1Mapping软件（MapIT software，SiemensHealthcare，Germany），程序自动生成两个不同的反转角而保持其他所有参数不变，连续进行两次扫描，则可自动生成T1Mapping图。

表2　MR扫描序列及参数

Table 2　MR scanning sequences and parameters

Parameterssequences	TR/ms	TE/ms	FA/°	Time	Range/mm	Thick-ness/mm	Matrix	FOV
T1WI								
Opp-phase	200	3.7	65	22.89 "	21	3	205×256	250×250
IR	1 240	2.5	9	24 "	28	4	768p×768	250×250
SE	400	10	80	4 ' 30 "	21	3	179p×256	250×250
T1-fl2d	225	2.5	70	24.17 "	21	3	256p×320	258×258
T1-vibe	4.4	1.6	13	30.28 "	80	1	240×320	250×250
T1-3D	2 000	2.7	9	8 ' 32 "	96	1	512×512	250×250
T1Mapping								
VIBE_Mapping	4.4	1.6	2,12	22 "	80	1	240×320	250×250
T1- 3D_Mapping	2 000	2.7	3,15	16 ' 46 "	80	1	448×640i	250×250
T1-fl2d_Mapping	225	2.5	30,70	48 "	21	3	240×320	250×250

TR：reverse time；TE：echo time；FA：flip angle；FOV：field of view；IR：inversion recovery；SE：spin echo；VIBE：volume interpolated body examination.

1.3　图像及数据分析

扫描结束后将所采集的图像传输至工作站（Siemens Leonardo Syngo 2009B）处理。T1WI中的测量数据：体模溶液信号强度Sp，同一层面踝关节肌肉信号强度Sm。T1Mapping扫描序列测量数据包括①体模溶液T1值T1p；②同一层面踝关节肌肉T1值T1m；③背景噪声水平T1n（测量层面靠近体模前、后、左、右方空气的噪声值水平的平均值）。

由2名有15年MR诊断经验医师分别进行数据测量，每个部位分别测量3次，并计算测量的平均值。感兴趣区（region of interest，ROI）的选择原则：尽可能接近体模管腔面积，并采用复制ROI的方法测量踝关节肌肉信号及邻近体模空气噪声值。肌肉信号测量选取与体模测量同一层面相近水平截面积最大的肌肉，避开T1WI显示的高信号脂肪间隙。

常规T1WI扫描序列计算相对信号强度（relative signal intensity，RSI），即体模信号强度（signal intensity，SI）与肌肉SI比值，算式S=Sp/Sm。各T1Mapping序列计算信噪比（signal to noise ratio，SNR），即体模T1值与背景噪声的比值，算式：SNR=T1p/T1n。对比噪声比（contrast noise ratio，CNR）为体模T1值与肌肉T1值的差值的绝对值与背景噪声的比值，算式：CNR= | T1p-T1m | /T1n。

使用SPSS 19.0 for Windows（Statistical Package for Social Science，Chicago，USA）统计软件进行统计学分析。采用Spearman检验比较各种常规T1WI扫描序列测定的SNR、CNR以及T1Mapping序列测定的T1值与对比剂浓度的相关性。用区组设计的方差分析及多重比较，分别比较三种T1Mapping序列所得图像的SNR、CNR的差异有无统计学意义。本研究中，均数置信区间设为95%，P值小于0.05被认为具有统计学有意义。

2 结 果

2.1 各种MR扫描序列测量信号强度与Gd-EOB-DTPA浓度的关系

各序列检查测定的体模SI很好地涵盖了人体各类组织的SI,而0.6的稀释比又不至于跨度过大,灰度分布及对比良好。随着对比剂浓度的减低,体模图像均逐渐由白变黑,SI逐渐减低,体模SI与Gd-EOB-DTPA浓度分布呈正相关,但不同的扫描序列直接测量的SI有较明显的差别(图2、3)。

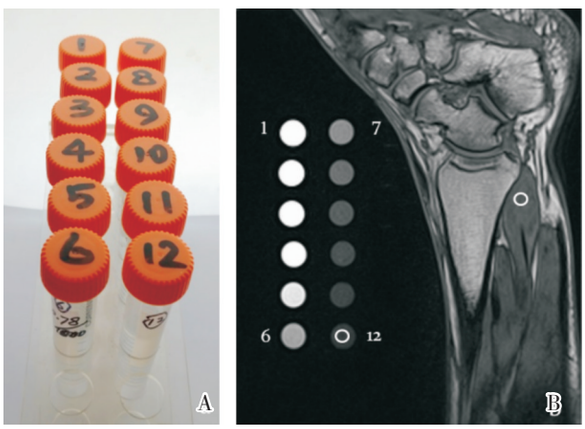

A: Gd-EOB-DTPA phantom was placed in the tube rack. The long axis of the rack was located in the center of the magnetic field and parallel to the main magnetic field. B: MR image acquired using T1-vibe sequence. The region of interest (ROI) was as close to the lumen area of the phantom as possible. The ROI of muscle was placed in the muscle with largest sectional area at the same level of the phantom.

图2 体模示意图及MR图像

Fig.2 Gd-EOB-DTPA phantom and MR image

采用Spearman检验比较各种常规T1WI扫描序列测定的SI,各序列测定的SI与对比剂浓度分布均呈正相关,且相关性均有统计学意义($P<0.05$)。从相关系数看三维容积内插体部检查(volume interpolated body examination, VIBE)序列及T1-3DX序列最好(表3)。

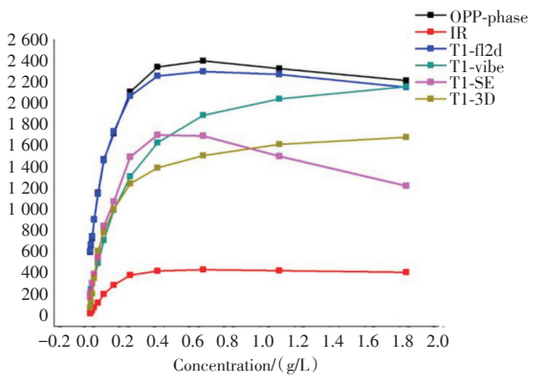

图3 常规T1WI扫描序列信号强度曲线

Fig.3 Signal intensity (SI) cures of conventional T1WI scanning sequences

2.2 各种MR扫描序列测量相对信号强度与Gd-EOB-DTPA浓度的关系

以志愿者踝关节肌肉SI为参照对比测量,绘制体模RSI(S1=Sp/Sm)曲线(图4)。RSI与Gd-EOB-DTPA浓度分布呈正相关。采用Spearman检验比较各种常规T1WI扫描序列测定的RSI,各序列测定相对信号强度与对比剂浓度分布相关性均有统计学意义($P<0.05$)。VIBE、T1-3D序列的相关性最好($R=1.000$;表4)。SI与RSI测定对评价对比剂浓度分布几乎没有差别。

2.3 各种T1Mapping扫描序列T1值与Gd-EOB-DTPA浓度的关系

利用T1Mapping软件,VIBE、T1-fl2d、T1-3D

表3 常规T1WI扫描序列测定的信号强度与Gd-EOB-DTPA浓度分布相关性

Table 3 Correlation between the signal intensity of traditional T1WI scan and the concentration distribution of Gd-EOB-DTPA solution

	Opp-phase	IR	T1-fl2d	T1-vibe	SE	T1-3D
Correlation coefficient	0.937	0.951	0.951	1.000	0.902	1.000
P	0.000	0.013	0.000	<0.001	0.000	<0.001
N	12	12	12	12	12	12

IR: inversion recovery; SE: spin echo; VIBE: volume interpolated body examination.

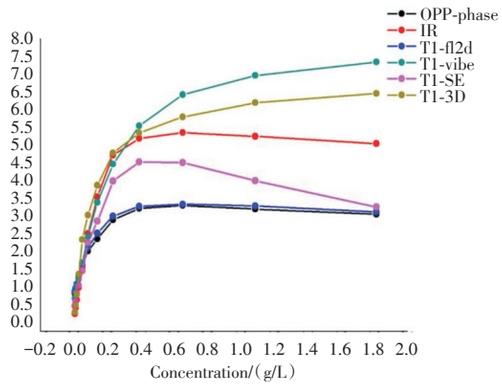

图4　常规T1WI扫描序列相对信号强度曲线

Fig.4　Relative signal intensity（RSI）cures of conventional T1WI scanning sequences

表4　常规T1WI扫描序列测定的相对信号强度与Gd-EOB-DTPA浓度分布相关性

Table 4　Correlation between the related signal intensity of traditional T1WI scan and the concentration distribution of Gd-EOB-DTPA solution

	Opp-phase	IR	T1-fl2d	T1-vibe	SE	T1-3D
R	0.937	0.951	0.951	1.000	0.902	1.000
P	0.000	0.000	0.000	< 0.001	0.000	< 0.001
n	12	12	12	12	12	12

IR：inversion recovery；SE：spin echo；VIBE：volume interpolated body examination.

均可获得体模T1图，在工作站上可以直接测量体模溶液、组织T1值（表5；图5）。

表5　各种T1Mapping扫描序列T1值

Table 5　T1 value from different T1Mapping scanning sequences

	VIBE_Mapping	T1-tra-3D_Mapping	T1-fl2d_Mapping
1	29.1	31.9	27.9
2	55.6	58.7	54.5
3	104.4	105.8	100.6
4	174.4	179	171.4
5	281	281.4	269.1
6	413.8	411.7	408.7
7	824.8	845.6	784.6
8	1 180	1 238.7	1 122.7
9	1 584.9	1 624.5	1 498.7
10	1 897.2	1 974.1	1 827.7
11	1 971.6	2 122.2	1 893.2
12	1 921.1	2 056.8	1 888.2

体模溶液T1值与Gd-EOB-DTPA浓度分布呈负相关，即Gd-EOB-DTPA浓度越高，T1值越低（图6）。不同的扫描序列所得T1值无明显差异。采用Spearman检验比较各T1Mapping序列测定T1值，可见三者相关系数相同，与Gd-EOB-DTPA浓度分布相关性均有统计学意义（P<0.05；表6）。

2.4　T1Mapping扫描序列图像质量比较

VIBE、T1-3D和T1-fl2d序列的SNR（F=102.214，P=0.000）、CNR（F=37.989，P=0.000）间具有统计学差异。VIBE序列的SNR、CNR均高于T1-3D、T1-fl2d（P<0.05），而T1-3D与T1-fl2d的SNR、CNR差别均无统计学意义（P>0.05；表7、8）。

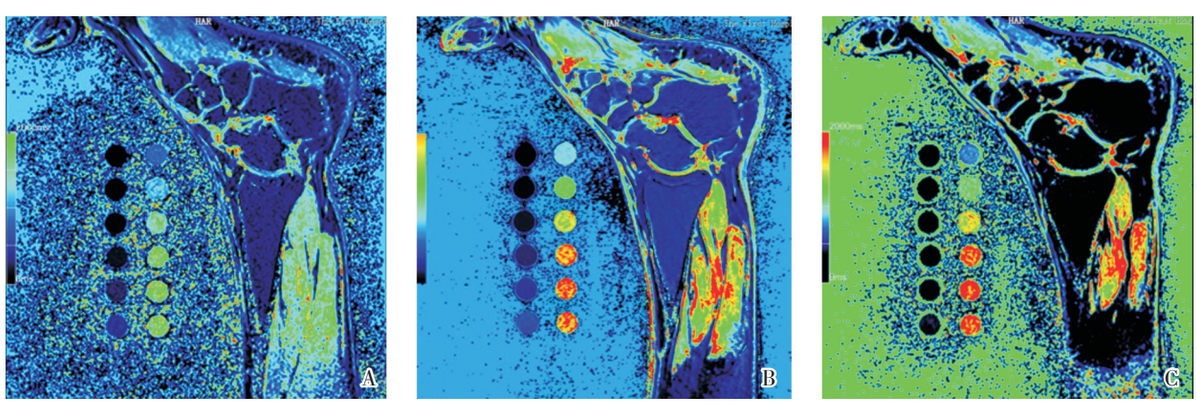

A：T1Mapping acquired using VIBE sequence；B：T1Mapping acquired using T1-fl2d sequence；C：T1Mapping acquired using T1-3D sequence.

图5　不同扫描序列获得的T1Mapping图

Fig.5　T1Mapping acquired using different sequences

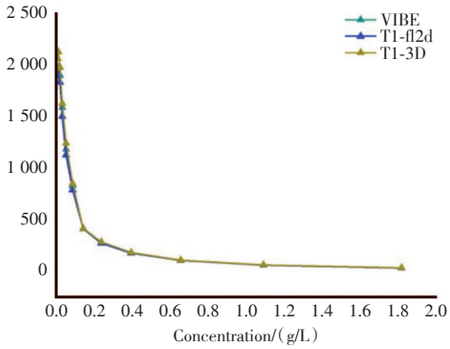

图6 各种T1Mapping序列测定T1值曲线

Fig.6 T1 value curves measured by different T1Mapping sequences

3 讨 论

Gd-EOB-DTPA应用于肝脏疾病评价时,RSI测定的方法往往采用肌肉或者脾脏作为SI对比测量[11-12]。由于肌肉的SI相对脾脏更稳定、均匀,是良好的参照物,故本实验采用健康志愿者踝关节肌肉作为参照,与体模测定的SI作为对比研究。

本研究中,各种常规T1WI扫描序列测定的信号强度与对比剂浓度分布相关性研究中,除SE序列外,其余各序列测定的SI及RSI变化曲线与对比剂浓度曲线均吻合。SI及RSI曲线中发现,SE序列在Gd-EOB-DTPA浓度更高的试管1-2信号SI及RSI反而低于试管3-4,可能与SE序列扫描时磁场的不均匀有关。上述结果表明,采用SI或RSI定量Gd-EOB-DTPA浓度容易出现较大的偏差。原因是T1WI检测到的信号强度不是组织

表6 T1Mapping扫描序列测定T1值与Gd-EOB-DTPA浓度分布相关性

Table 6 Correlation between the T1 value from different T1Mapping scanning sequences and the concentration distribution of Gd-EOB-DTPA solution

	VIBE_Mapping	T1-3D_Mapping	T1-fl2d_Mapping
Correlation Coefficient	-0.993	-0.993	-0.993
P	0.000	0.000	0.000
n	12	12	12

表7 T1Mapping序列图像的信噪比、对比噪声比

Table 7 The Signal to Noise Ratio(SNR) and contrast noise ratio(CNR) of T1Mapping sequences

T1Mapping	SNR	CNR	*N*
VIBE	1.62±1.48	1.62±1.01	12
T1-3D	1.33±1.24	1.27±0.67	12
T1-fl2d	1.18±1.08	1.17±0.71	12
Total	1.38±1.25	1.36±0.81	36

SNR: signal to noise ratio; CNR: contrast noise ratio; VIBE: volume interpolated body examination.

表8 T1Mapping序列图像的信噪比、对比噪声比的多重比较

Table 8 Multiple comparison of the Signal to Noise Ratio(SNR) and contrast noise ratio(CNR) of T1Mapping sequences

Sequences	P_{SNR}	P_{CNR}
VIBE T1-3D	0.002	0.000
VIBE T1-fl2d	0.000	0.000
T1-3D T1-fl2d	0.082	0.296

SNR: signal to noise ratio; CNR: contrast noise ratio; VIBE: volume interpolated body examination.

固有的T1值[13]，不仅受到主磁场的影响，还受到脉冲序列、成像参数、射频放大器的增益等的影响，其测量值的直接比较会带来较大的误差[6,7]。

因此，要对Gd-EOB-DTPA的分布情况进行准确的评估及比较，必须测定组织的T1弛豫时间。组织的T1值测定往往需要改变某个参数来获得2组或2组以上的图像，各次扫描必须保持目标参数外所有成像参数及解剖位置一致[14]。但在体部扫描中因为容易受呼吸等运动的影响，很难做到解剖位置不变[15-16]。既往T1值测定主要是利用SE或IR两种序列[14,17-19]，改变TR或TI，保持其他参数不变，测量不同图像上组织的信号强度，利用复杂的公式计算T1值。但这些方法存在费时、容易产生呼吸伪影、误差较大等缺点。

目前已经研发出先进的T1Mapping软件[20]，自动计算各个像素的T1值并能合成组织的T1图，能方便快捷地获得组织的T1图。本研究使用Magnetom Verio 3.0T超导MRI扫描仪的三种常用T1WI序列：VIBE、T1-3D、T1-fl2d，均可获得T1图，可以直接测量体模溶液、组织T1值。从各T1Mapping序列测定T1值曲线可以看到，体模溶液T1值与Gd-EOB-DTPA浓度分布呈负相关，即Gd-EOB-DTPA浓度越高，T1值越低。不同扫描序列所得T1值没有明显的差异。采用Spearman检验比较各T1Mapping序列测定T1值，三者相关系数相同，与Gd-EOB-DTPA浓度分布相关性均有统计学意义。在三者的图像质量比较中，VIBE序列SNR、CNR均高于T1-3D、T1-fl2d，而T1-3D与T1-fl2d序列的SNR、CNR差别均无统计学意义，由此可见，VIBE序列获得的T1图质量更好。

T1值的测量过程中影响结果的主要因素是图像的信噪比。而其他的一些因素，如：梯度场的不准确、涡流（eddy current）以及射频激发的不均匀性、不准确性亦可能对测量产生影响[14]。因此，使用VIBE序列进行T1Mapping测定能获得更稳定可靠的结果。更重要的是，在扫描所需时间上，VIBE序列以不同反转角两次扫描获得体模长80 mm层厚1 mm的T1Mapping图仅需22 s，T1-fl2d序列获得体模长21mm的T1Mapping图需要48 s，而T1-3D序列获得体模长80 mm层厚1 mm的T1Mapping图更是需要16 m 46 s。因此，在临床肝脏检查应用中，T1-fl2d序列特别是T1-3D序列难以避免呼吸运动的影响而获得满意的T1图。

本研究证实了T1Mapping软件能准确测量Gd-EOB-DTPA体模的T1值。在T1Mapping的各种序列中，VIBE序列扫描速度快，在层面很薄时仍然保持着很高的信噪比，更适用于Gd-EOB-DTPA肝脏增强MR检查。

参考文献

[1] Kim S, Shin J, Kim DY, et al. Radiomics on gadoxetic acid-enhanced magnetic resonance imaging for prediction of postoperative early and late recurrence of single hepatocellular carcinoma[J]. Clin Cancer Res, 2019, 25(13):3847-3855.

[2] Getzin T, Gueler F, Hartleben B, et al. Gd-EOB-DTPA-enhanced MRI for quantitative assessment of liver organ damage after partial hepatic ischaemia reperfusion injury: correlation with histology and serum biomarkers of liver cell injury[J]. Eur Radiol, 2018, 28(10):4455-4464.

[3] Kim HD, Lim YS, Han S, et al. Evaluation of early-stage hepatocellular carcinoma by magnetic resonance imaging with gadoxetic acid detects additional lesions and increases overall survival[J]. Gastroenterology, 2015, 148(7):1371-1382.

[4] Kim AY, Sinn DH, Jeong WK, et al. Hepatobiliary MRI as novel selection criteria in liver transplantation for hepatocellular carcinoma[J]. J Hepatol, 2018, 68(6):1144-1152.

[5] Zhu WS, Shi SY, Yang ZH, et al. Radiomics model based on preoperative gadoxetic acid-enhanced MRI for predicting liver failure[J]. World J. Gastroenterol, 2020, 26(11):1208-1220.

[6] Kim JE, Kim HO, Bae K, et al. T1 mapping for liver function evaluation in gadoxetic acid-enhanced MR imaging: comparison of look-locker inversion recovery and B 1 inhomogeneity-corrected variable flip angle method[J]. Eur Radiol, 2019, 29(7):3584-3594.

[7] Luetkens JA, Klein S, Träber F, et al. Quantification of liver fibrosis at T1 and T2 mapping with ex-

tracellular volume fraction MRI: preclinical results [J]. Radiology, 2018, 288(3):748-754.
[8] Zhou ZP, Long LL, Qiu WJ, et al.Evaluating segmental liver function using T1 mapping on Gd-EOB-DTPA-enhanced MRI with a 3.0 Tesla [J]. BMC Med Imaging, 2017, 17(1):20.
[9] Yoon JH, Lee JM, Paek M, et al. Quantitative assessment of hepatic function: modified look-locker inversion recovery (MOLLI) sequence for T1 mapping on Gd-EOB-DTPA-enhanced liver MR imaging[J]. Eur Radiol, 2016, 26(6):1775-1782.
[10] Friedman L, Glover GH. Report on a multicenter fMRI quality assurance protocol [J]. J Magn Reson Imaging, 2006, 23(6):827-839.
[11] Sheng RF, Wang HQ, Yang L, et al. Assessment of liver fibrosis using T1 mapping on Gd-EOB-DTPA-enhanced magnetic resonance [J]. Dig Liver Dis, 2017, 49(7):789-795.
[12] Yoon JH, Lee JM, Kim E, et al. Quantitative liver function analysis: volumetric T1 mapping with fast multisection B1 inhomogeneity correction in hepatocyte-specific contrast-enhanced liver MR imaging [J]. Radiology, 2017, 282(2):408-417.
[13] Taylor AJ, Salerno M, Dharmakumar R, et al. T1 mapping: basic techniques and clinical applications [J]. JACC Cardiovasc Imaging, 2016, 9(1):67-81.
[14] Fernandes JL, Rochitte CE. T1 mapping: technique and applications [J]. Magn Reson Imaging Clin N Am, 2015,23(1):25-34.
[15] Yoo JL, Lee CH, Park YS, et al. The shortbreath-hold technique, controlled aliasing in parallel imaging results in higher acceleration, can be the first step to overcoming a degraded hepatic arterialphase in liver magnetic resonance imaging: a prospective randomized controlstudy[J]. Invest Radio, 2016,51(7):440-446.
[16] Yang S, Shan F, Yan Q, et al. A pilot study of native T1-mapping for focal pulmonary lesions in 3.0 T magnetic resonance imaging: size estimation and differential diagnosis [J]. J Thorac Dis, 2020, 12(5):2517-2528.
[17] Dekkers IA, de Boer A, Sharma K, et al. Consensus-based technical recommendations for clinical translation of renal T1 and T2 mapping MRI [J]. MAGMA, 2020, 33(1):163-176.
[18] Jiang K, Zhu Y, Jia S, et al. Fast T1 mapping of the brain at high field using Look-Locker and fast imaging [J]. Magn Reson Imaging, 2017, 36:49-55.
[19] Tran-Gia J, Bisdas S, Köstler H, et al. A model-based reconstruction technique for fast dynamic T1 mapping[J]. Magn Reson Imaging, 2016, 34(3):298-307.
[20] Wang WT, Zhu S, Ding Y, et al. T1 mapping on gadoxetic acid-enhanced MR imaging predicts recurrence of hepatocellular carcinoma after hepatectomy [J]. Eur J Radiol, 2018, 103:25-31.

(编辑 余 菁)